nature geoscience

LETTERS

PUBLISHED ONLINE: 20 NOVEMBER 2011 | DOI: 10.1038/NGEO1325

Recent contribution of sediments and fluids to the mantle's volatile budget

Simon Turner[1]*, John Caulfield[1], Michael Turner[1], Peter van Keken[2], René Maury[3], Mike Sandiford[4] and Gaelle Prouteau[5]

Subduction modifies the cycling of Earth's volatile elements. Fluid-rich sediments and hydrated oceanic lithosphere enter the convecting mantle at subduction zones. Some of the sediments and volatile components are released from the subducting slab, promote mantle melting and are returned to the surface by volcanism. The remainder continue into the deeper mantle. Quantification of the fate of these volatiles requires an understanding of both the nature and timing of fluid release and mantle melting[1]. Here we analyse the trace element and isotopic geochemistry of fragments of upper mantle rocks that were transported to the surface by volcanic eruptions above the Batan Island subduction zone, Philippines. We find that the mantle fragments exhibit extreme disequilibrium between their U–Th–Ra isotopic ratios, which we interpret to result from the interaction of wet sediment melts and slab-derived fluids with rocks in the overlying mantle wedge. We infer that wet sediments were delivered from the slab to the mantle wedge between 8,000 and 10,000 years ago, whereas aqueous fluids were delivered separately much later. We estimate that about 625 ppm of water is retained in the wedge. A significant volume of water could therefore be delivered to the mantle transition zone at the base of the upper mantle, or even to the deeper mantle.

As fluids and melts rise from subducting slabs they may interact with each other and the surrounding mantle wedge and may be contaminated or modified by shallow processes such as cumulate melting and crystal fractionation. To separate the role of these possible, contributing processes we need to constrain physical processes. A significant number of short-lived (U-series) isotopes studies have been conducted on arc lavas and magma chamber residence times are quite well constrained[2]. However, conclusions about the timing of source metasomatism have varied (1–100 kyr; refs 2–6) and there has been debate about the extent to which these signals reflect processes of fluid addition and partial melting. Alternative interpretations have included steady-state diffusion in the mantle wedge[7] or even shallow-level processes, such as surface contamination[8] and crustal melting[9]. It has also been suggested that correlations between key trace element ratios and U-series disequilibria may largely reflect magma differentiation and ageing[10].

These issues have predominantly been tackled indirectly by interrogating the geochemical signatures of arc lavas. However, it has also been suggested that some rare, metasomatized, mantle xenoliths, such as those occurring on Batan Island in the Philippines (Fig. 1), may provide direct information on processes occurring in the sub-arc mantle wedge[11–13], although there has been debate over whether their metasomatic signatures reflect addition of aqueous fluids or slab melts[13–15]. Here, we report the first measurements of ^{238}U–^{230}Th–^{226}Ra isotopes, along with whole rock and mineral compositions, from six mantle xenoliths and two samples of their host lava from Iraya volcano on Batan Island. All exhibit significant disequilibria, providing the first direct evidence both for the nature and timing of metasomatism in the sub-arc mantle.

Details about the samples used, including mineral modes, are given in the Methods section. The xenoliths do not themselves show signs of partial melting, but olivine melt inclusions contain 57–63 wt% SiO_2 and 4.4–5.2 wt% H_2O (ref. 13). Our Fourier transform infrared (FTIR) spectroscopy indicates that visually unaltered orthopyroxene also contains significant amounts (625 ppm) of H_2O (Fig. 2b). These combined data are consistent with the formation of up to 20% of the total orthopyroxene by replacement of olivine during metasomatism by a wet silicic sediment melt[13,16].

The orthopyroxene-rich nature of the xenoliths precludes their origin as cumulates, but their depth of origin has never been fully addressed. Two-pyroxene thermometry from the xenoliths yields temperatures of 900–1,100 °C (ref. 16) and the presence of hydrous minerals and significant amounts of water in melt inclusions and orthopyroxene suggest that the peridotite dehydration solidus has not been crossed. That, and the absence of garnet, constrains the upper limit of temperature and pressure to less than 1,100 °C and 3 GPa, respectively (Fig. 2c). To obtain further constraints, we developed a model for the thermal structure of this subduction zone based on recent geodynamical models[17]. The only region below the arc that is at sufficiently high temperature lies between 1.5 and 3 GPa (Fig. 2c), which indicates that the xenoliths may be derived from the asthenosphere.

Our new geochemical and isotopic data (Supplementary Table S1) are illustrated along with previously published data for the lavas on Figs 3 and 4. The xenoliths are enriched in MgO (43–48 wt%), Ni (2,715–3,152 ppm) and Cr (2,049–3,897 ppm). They have very similar incompatible trace element patterns to their host lavas[11], albeit with lower concentrations (Fig. 3a), and arc lavas in general. Subtle differences, such as observed for Zr–Hf in sample Song 24b, probably reflect variations in the relative fluid and sediment component contributions. On a plot of Sr/Th versus Th/Ce, mafic arc lavas typically form a curved array extending to high Sr/Th at low Th/Ce and elevated Th/Ce at low Sr/Th (Fig. 3b). The widely accepted interpretation is that the elevated Sr/Th endmember reflects large contributions from an aqueous fluid component whereas the elevated Th/Ce component

[1]Department of Earth and Planetary Sciences, Macquarie University, Sydney, New South Wales 2109, Australia, [2]Department of Geological Sciences, University of Michigan, Michigan 48109-1005, USA, [3]UMR CNRS 6538 Domaines Océaniques, Universite de Bretagne Occidentale, BP 809, 29285 Brest, France, [4]School of Earth Sciences, University of Melbourne, Melbourne, Victoria 3010, Australia, [5]Université Pierre et Marie Curie, Laboratoire de Pétrologie, 4 Place Jussieu, Paris cedex 05, France. *e-mail: simon.turner@mq.edu.au.

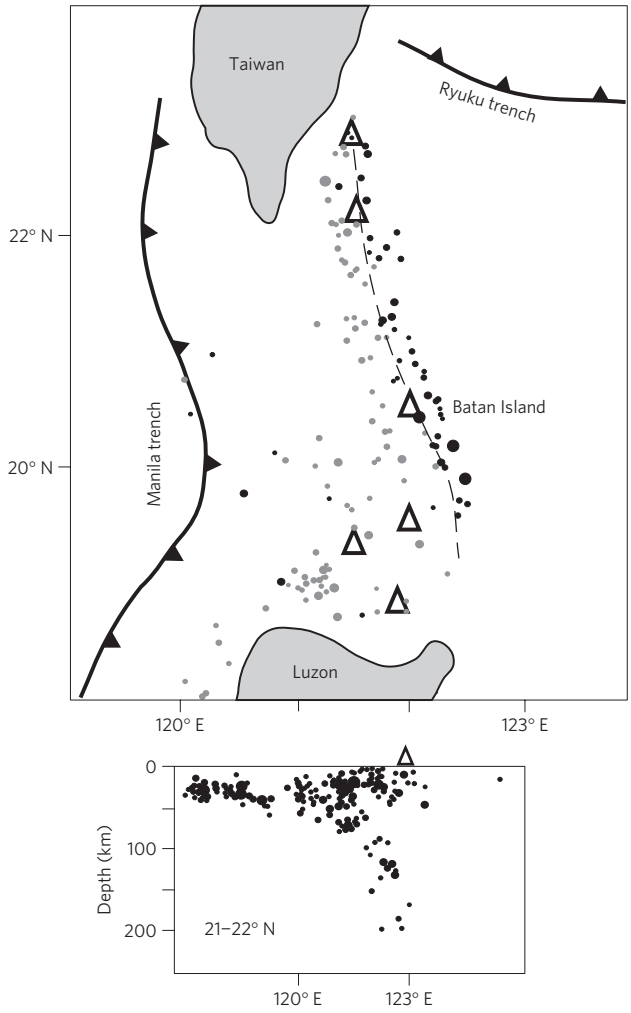

Figure 1 | Physical setting of Batan Island. Batan Island belongs to the least evolved segment of the Luzon arc and is located on oceanic crust at the northern end of the Philippine Sea plate. Volcanism reflects east-directed subduction of the South China Sea plate through the Manila trench and possible slab-tearing. Intermediate-depth earthquake solutions, shown as dots, are inclusive to 2007. Location data are from the Engdahl–Hilst–Buland (EHB) Bulletin comprising the International Seismological Institute (ISC) Bulletin, groomed using the Engdahl *et al.*[28] algorithm to improve hypocentre locations (http://www.isc.ac.uk/EHB/index.html). Dashed line is the interpolated 100 km depth to slab contour. The grey circles indicate earthquakes located at depths between 60 and 100 km; the black circles are greater than 100 km. The size of a dot reflects the magnitude of an earthquake. Triangle indicates the position of a volcano. Lower panel shows a cross-section close to Batan Island.

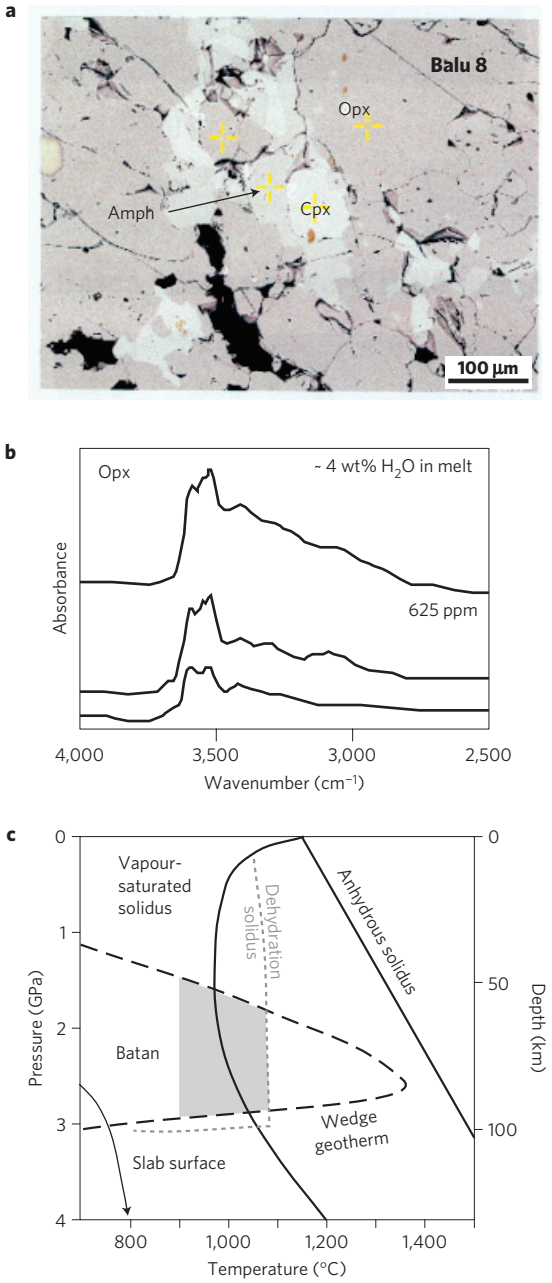

Figure 2 | Mineralogy, water content and pressure–temperature conditions of the xenoliths. a, SEM image showing interlocking clinopyroxene (Cpx), amphibole (Amph) and orthopyroxene (Opx) (black grains are Cr-spinel). **b**, FTIR spectra and inferred water contents for orthopyroxene. **c**, Pressure–temperature diagram constraining the origin of the xenoliths (grey field) by combining their inferred temperatures[16] with a calculated wedge geotherm and the location of the peridotite dehydration solidus; phase boundaries from ref. 29. The wedge geotherm was based on the D80 model[17], assuming a potential temperature of 1,350 °C, a convergence rate of 7 cm yr^{-1}, and slab dip and depth to slab as determined from the seismic data shown on Fig. 1.

reflects additions from a sediment and, possibly, sediment melt[18]. Strikingly, the Batan xenoliths exactly mimic this global arc array (Fig. 3b) and the low Sr/Th, high Th/Ce xenoliths extend to elevated $^{87}Sr/^{86}Sr$ consistent with a sediment influence (inset to Fig. 3b). Note that, although Philippine lavas (including those from Batan Island) also contain evidence for addition of both fluid and sediment components to the mantle wedge[19], they exhibit a much more restricted compositional range than the xenoliths or lavas from more depleted arcs.

The U-series disequilibria are shown on Fig. 4 and again encompass much of the global range observed in mafic arc lavas ($SiO_2 < 60$ wt%). Consistent with previous data[19,20], the Batan (and other Philippine) lavas are close to ^{238}U–^{230}Th secular equilibrium and are characterized by low ($^{230}Th/^{232}Th$) ratios relative to most arc lavas[2]. This precludes host lava contamination as the cause of the disequilibria in the xenoliths because these preserve large U–Th disequilibria ranging from ($^{230}Th/^{238}U$) = 0.55 to 1.92 (Fig. 4a). Moreover, the ($^{226}Ra/^{230}Th$) ratios of the xenoliths extend from within error of secular equilibrium, in those xenoliths with excess of ^{230}Th over ^{238}U, up to ($^{226}Ra/^{230}Th$) = 7.5, in those with ^{238}U excess (Fig. 4b). The latter value is higher than any yet reported

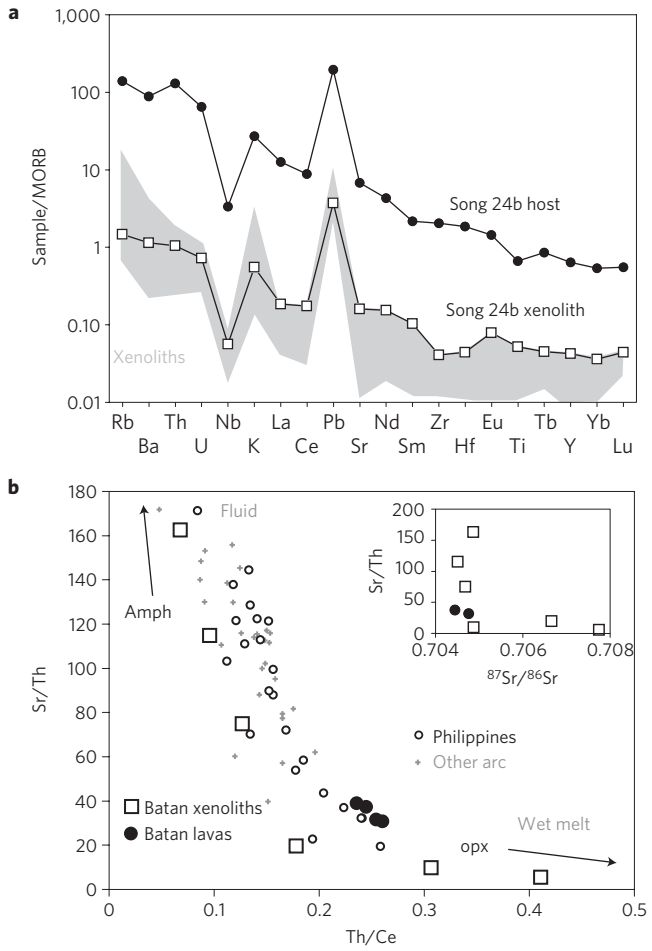

Figure 3 | Trace element characteristics of the xenoliths. a, Incompatible trace element diagram highlighting the similarity between the xenoliths (grey field indicates range) and host lava(s). **b**, Plot of Sr/Th versus Th/Ce showing the xenoliths mirror the global arc field, shown as small grey crosses[2], including Batan and other Philippine lavas[19,20], along with inset of Sr/Th versus $^{87}Sr/^{86}Sr$. Elevated Sr/Th is indicative of an aqueous fluid component and also characterizes the hydrous minerals in the xenoliths (Supplementary Table S1). Elevated Th/Ce and $^{87}Sr/^{86}Sr$ is indicative of contributions from a sediment component, but also a feature of the orthopyroxene in the xenoliths inferred to have been formed by metasomatism of pre-existing olivine by a wet, siliceous melt.

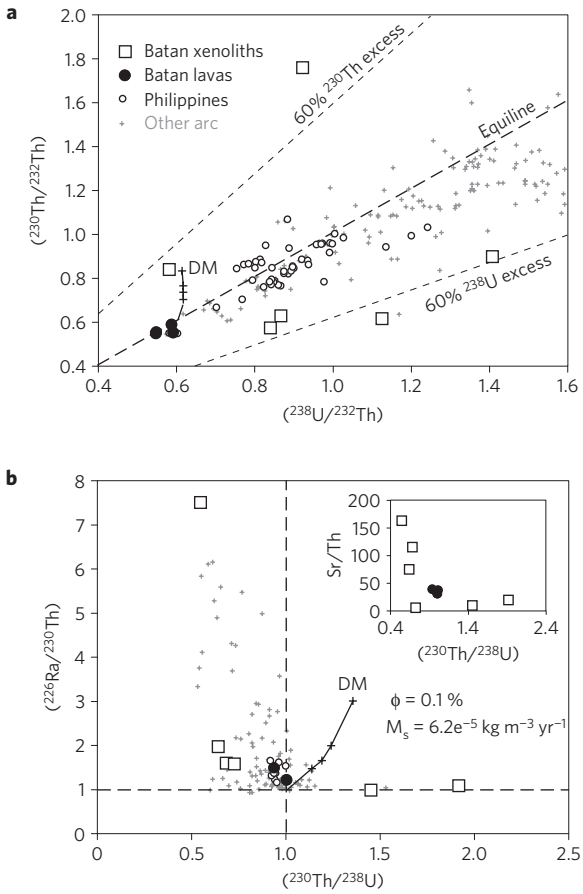

Figure 4 | U-series disequilibria in the xenoliths. a, $(^{230}Th/^{232}Th)$ versus $(^{238}U/^{232}Th)$ and **b**, $(^{226}Ra/^{230}Th)$ versus $(^{230}Th/^{238}U)$ showing that the disequilibria in the xenoliths overlap the Batan lavas, other Philippine lavas[19,20] and the global arc field (shown as small grey crosses; data compilation from ref. 2). The dynamic melting curve (labelled DM and based on ref. 30) illustrates the trajectory of melts produced by peridotite melting in the absence of metasomatism by slab-derived fluids (that is reducing conditions). Inset on **b** shows Sr/Th versus $(^{230}Th/^{238}U)$. Error bars are smaller than the symbols, see text for discussion.

from arc lavas. Given that the xenoliths must be at least 1,480 yr old, implies an initial $(^{226}Ra/^{230}Th)$ ratio ~14, similar to some theoretical estimates for the maximum $(^{226}Ra/^{230}Th)$ ratio likely to be encountered in slab fluids[2].

In our preferred interpretation, the isotopic and trace element characteristics of the xenoliths reflect, and thereby constrain the nature and timing of, metasomatism of the sub-arc mantle wedge. Steady state diffusion is conceivable on the grain scale[7], but would not be expected to produce such extreme and differing senses of disequilibria on the hand-specimen scale (1–2 cm). Nor would *in situ* partial melting of the xenoliths during ascent[21]. The xenoliths are clearly of mantle origin, precluding models invoking crustal melting[9] or crystal fractionation[10] and suggesting such models are equally not required to explain similar signatures that are commonly observed in arc lavas. As illustrated by the numerical melt model shown on Fig. 4a,b, dynamic melting of peridotite, in the absence of metasomatism (that is, normal mantle oxygen fugacity), produces coupled ^{230}Th and ^{226}Ra excesses that are not a feature of the xenolith suite. Furthermore, none of the above processes provides a good explanation for the Sr/Th–Th/Ce correlation either. Instead, this correlation is well explained by metasomatism. The component with ^{238}U and ^{226}Ra excess has low $^{87}Sr/^{86}Sr$ and elevated Sr/Th, typical of that inferred for an aqueous fluid from the altered basaltic component of the subducting slab. We note that amphibole (probably formed by reaction of clinopyroxene with such fluids) in these xenoliths can have Sr/Th > 4,600 with Th/Ce ~ 0 (Supplementary Table S1). The large ^{226}Ra disequilibria require that this was added within the past few millennia and potentially could have been on-going at the time of entrainment in the host lavas.

The other geochemical endmember has ^{230}Th excess over ^{238}U without ^{226}Ra excess as well as elevated Th/Ce and $^{87}Sr/^{86}Sr$ and these features are not characteristic of likely melts of the subducted oceanic crust. However, a number of studies have suggested that the overlying sediment component might be added as a melt[1,5] in which residual accessory phases[1] might lead to significant disequilibria. For example, a recent study has suggested that negative Zr–Hf anomalies probably reflect the presence of residual zircon[22] which could produce the ^{230}Th excess. Therefore this endmember is inferred to reflect a sediment contribution, and its trace element signature is best developed in the orthopyroxenes that have Sr/Th < 25 and Th/Ce > 0.6 (Supplementary Table S1).

The nature of the orthopyroxenes, discussed above, is consistent with this metasomatic agent being a wet, siliceous melt of sediment. The combination of ^{230}Th excess and ^{226}Ra equilibrium suggest that addition of this component occurred earlier (possibly from deeper, hotter slab conditions), between 8 kyr and potentially a few tens of kyr. It seems likely that we have resolved the aqueous fluids versus slab melts debate[13–15] by showing that both components are involved.

The most profound result of our study is that these Batan xenoliths provide the first direct evidence for both the nature and timing of sub-arc metasomatism (that is, as opposed to those inferred from arc lavas). Clearly, source U-series signatures could potentially be overprinted by the effects of in-growth melting and further modified by magma differentiation and ageing. However, the similar and overlapping trace element—U-series correlations observed in both the xenoliths and lavas provide encouragement that such signatures in arc lavas faithfully reflect signatures derived from the mantle (that is, they are not overwhelmed by subsequent processes). It is likely that the xenoliths came from depths above the source of the lavas and thus provide an analogue for the source of the lavas rather than being samples of the source themselves. Melting of mantle (including the effects of U-series nuclide in-growth) with such a range of compositions would homogenize much of the extremities of local heterogeneity and we suggest this is the reason the xenoliths (and their constituent minerals) preserve a much greater range of trace element variability and U-series disequilibria than their host lavas.

Nevertheless, a number of outstanding questions remain. Where and how did the host lavas differentiate? Under what conditions can a (^{230}Th/^{238}U) ratio of 1.92 develop in harburgite? Could residual zircon[22] sufficiently retain U relative to Th? In detail, the composition and mineralogy of each individual xenolith is complex and the effects of metasomatism are likely to have a strong mineralogical control in addition to the relative proportions of fluid versus sediment added to them. Unfortunately, sample sizes prevented determination of mineral modes in all of the xenoliths (see Methods section). Nevertheless, sample Song 3a contains significantly more amphibole than sample Balu 8 and this sample also has higher Sr/Th, lower ^{87}Sr/^{86}Sr and larger ^{238}U and ^{226}Ra excesses. Such signatures are all entirely consistent with a greater relative aqueous fluid contribution and with the high Sr/Th ratios of the amphiboles (Supplementary Table S1).

Last, the xenoliths have >20% orthopyroxene containing 625 ppm H_2O, olivine full of inclusions with 4–5 wt% H_2O (ref. 13) as well as amphibole and/or phlogopite. Thus, 625 ppm probably provides a minimum estimate of the amount of water contained in sub-Philippine mantle wedge peridotite. If this avoids partial melting it will be convected back into the deeper mantle, perhaps to the transition zone or beyond, where some mantle plumes are sourced. Alternatively, the suggestion that the solubility of H_2O in orthopyroxene decreases with increasing pressure[23] raises the possibility that this water becomes released. This could trigger small degree melts or form a separate fluid phase, either of which could be critical for explaining the seismic low-velocity zone. Such possibilities highlight the potential of further studies of U-series disequilibria in mantle xenolith suites to contribute to our understanding of mantle dynamics.

Methods

The xenoliths analysed come from sea cliffs at Songsong and Balugan bays where they are found as inclusions in basaltic-andesite pyroclastics and lavas with a ^{14}C age of 1,480 yr BP on associated fossil wood[24]. They are amphibole- and sometimes phlogopite-bearing harzburgites with medium- to coarse-grained textures (Fig. 2a), although sheared and non-hydrous mineral-bearing examples also exist[16]. Many are mantled by kaersutitic amphibole[12]. In turn, these amphibole rims are occasionally mantled by gabboric rims. In the latter case, the minerals from the gabbro have compositions identical to those of the host lava phenocrysts. Kaersutites from the inner rim have Mg# intermediate between those of the phenocrysts/gabbros and the xenolith amphiboles[24]. Mineral modes for our samples are typical of this locality[16]. Samples Song 24b, Song 3a and Balu 8 consist of olivine, orthopyroxene, clinopyroxene and amphibole in the following proportions: 65:27:4:4, 67:23:3:2 and 70:25:3:6, respectively. All samples contain small amounts of chrome spinel (Cr# 43–53).

Infrared spectra are from a sample with 0.45 mm average thickness. Individual measurements on nine unorientated crystals were analysed and averaged to obtain the spectra from which water contents were calculated. Mineral water contents (in ppm) are calculated using the absorbance coefficient from ref. 25. Correlation of water partitioning between pyroxene and melt, and proportion of tetrahedral site occupied by $Al^{IV}/(IV)_T$, as determined by ref. 26, was used to calculate the approximate water content of the melt (that is, ~4 wt%). Six 1–2 cm diameter xenoliths were prepared by removing all traces of adhering host lava and ultrasonicated in milli-Q water before powdering in an agate mill. Major elements were analysed on a Siemens SRS300 XRF at the University of Auckland; all other analyses were undertaken in the Geochemical Analysis Unit at Macquarie University. Mineral compositions were determined using a Cameca SX100 microprobe using a 10 μm spot size, accelerating voltage of 15 keV and beam current of 20 nA. Procedures used for both solution and LA–ICP–MS trace element analysis and the Sr, Nd and U-series measurements are described in detail in ref. 27. Results for BHVO-2 indicate that the accuracy of the trace element concentrations is better than 5%. Repeat analyses of BHVO-2 gave ^{87}Sr/^{86}Sr = 0.703498 ± 6 (n = 15) and ^{143}Nd/^{144}Nd = 0.512975 ± 3 (n = 17). The Table Mountain Latite standard (TML-3) yielded (^{230}Th/^{238}U) = 1.004 ± 5 (n = 5) and (^{226}Ra/^{230}Th) = 0.992 ± 6 (n = 4) and conservative long-term estimates of the reproducibility of these ratios are 2 and 6%, respectively. One of the host lavas and two of the xenoliths have (^{234}U/^{238}U) outside of analytical error (±0.8% 2σ) of secular equilibrium, potentially indicating some subsolidus contamination or alteration of these samples. However, there is no correlation between (^{234}U/^{238}U) and either (^{230}Th/^{238}U) or (^{226}Ra/^{230}Th), and the primary conclusions hold irrespective of whether these samples are included or not.

Received 11 January 2011; accepted 19 October 2011; published online 20 November 2011

References

1. Plank, T., Cooper, L. B. & Manning, C. E. Emerging geothermometers for estimating slab surface temperatures. *Nature Geosci.* **16,** 611–615 (2009).
2. Turner, S., Bourdon, B. & Gill, J. Insights into magma genesis at convergent margins from U-series isotopes. *Rev. Mineral. Geochem.* **52,** 255–315 (2003).
3. Gill, J. B., Morris, J. D. & Johnson, R. W. Timescale for producing the geochemical signature of island arc magmas: U–Th–Po and Be–B systematics in Recent Papua New Guinea lavas. *Geochim. Cosmochim. Acta* **57,** 4269–4283 (1993).
4. Reagan, M. K., Morris, J. D., Herrstrom, E. A. & Murrell, M. T. Uranium series and beryllium isotope evidence for an extended history of subduction modification of the mantle below Nicaragua. *Geochim. Cosmochim. Acta* **58,** 4199–4212 (1994).
5. Elliott, T., Plank, T., Zindler, A., White, W. & Bourdon, B. Element transport from slab to volcanic front at the Mariana arc. *J. Geophys. Res.* **102,** 14991–15019 (1997).
6. Turner, S., Evans, P. & Hawkesworth, C. Ultra-fast source-to-surface movement of melt at island arcs from ^{226}Ra–^{230}Th systematics. *Science* **292,** 1363–1366 (2001).
7. Feineman, M. D. & DePaolo, D. J. Steady-state ^{226}Ra/^{230}Th disequilibrium in mantle minerals: Implications for melt transport rates in island arcs. *Earth Planet. Sci. Lett.* **215,** 339–355 (2003).
8. Villemant, B., Boudon, G. & Komorowski, J. C. U-series disequilibrium in arc magmas induced by water-magma interaction. *Earth Planet. Sci. Lett.* **140,** 259–267 (1996).
9. Dufek, J. & Cooper, K. M. ^{226}Ra/^{230}Th excess generated in the lower crust: Implications for magma transport and storage time scales. *Geology* **33,** 833–836 (2005).
10. Huang, F., Gao, L. & Lundstrom, C. C. The effect of assimilation, fractional crystallisation, and ageing on U-series disequilibria in subduction zone lavas. *Geochim. Cosmochim. Acta* **72,** 4136–4145 (2008).
11. Maury, R. C., Defant, M. J. & Joron, J. L. Metasomatism of the sub-arc mantle inferred from trace elements in Philippine xenoliths. *Nature* **360,** 661–663 (1992).
12. Vidal, Ph., Dupuy, C., Maury, R. & Richard, M. Mantle metasomatism above subduction zones: Trace-element and radiogenic isotope characteristics of peridotite xenoliths from Batan Island (Philippines). *Geology* **17,** 1115–1118 (1989).
13. Schiano, P. *et al.* Hydrous, silica-rich melts in the sub-arc mantle and their relationships with erupted arc lavas. *Nature* **377,** 595–600 (1995).
14. Sajona, F. G. *et al.* Slab melt as metasomatic agent in island arc magma mantle sources, Negros and Batan (Philippines). *Island Arc* **9,** 472–486 (2000).

15. Eiler, J. M., Schiano, P., Valley, J. W., Kita, N. T. & Stolper, E. M. Oxygen-isotope and trace element constraints on the origins of silica-rich melts in the subarc mantle. *Geochem. Geophys. Geosyst.* **8,** Q09012 (2007).
16. Arai, S., Takada, S., Ashi, K. M. & Kida, M. Petrology of peridotite xenoliths from Iraya volcano, Philippines, and its implication for dynamic mantle-wedge processes. *J. Petrol.* **45,** 369–389 (2004).
17. Syracuse, E. M., van Keken, P. E. & Abers, G. A. The global range of subduction zone thermal models. *Phys. Earth Planet. Inter.* **183,** 73–90 (2010).
18. Hawkesworth, C. J., Turner, S. P., McDermott, F., Peate, D. W. & van Calsteren, P. U–Th isotopes in arc magmas: Implications for element transfer from the subducted crust. *Science* **276,** 551–555 (1997).
19. McDermott, F., Defant, M. J., Hawkesworth, C. J., Maury, R. C. & Joron, J. L. Isotope and trace element evidence for three component mixing in the genesis of the North Luzon arc lavas (Philippines). *Contrib. Mineral. Petrol.* **113,** 9–23 (1993).
20. DuFrane, S. A., Asmerom, Y., Musaka, S. B., Morris, J. D. & Dreyer, B. M. Subduction and melting processes inferred from U-series, Sr–Nd–Pb isotope, and trace element data, Bicol and Bataan arcs, Philippines. *Geochim. Cosmochim. Acta* **70,** 3401–3420 (2006).
21. Yaxley, G. M. & Kamenetsky, V. *In situ* origin for glass in mantle xenoliths from southeastern Australia: Insights from trace element compositions of glasses and metasomatic phases. *Earth Planet. Sci. Lett.* **172,** 97–109 (1999).
22. Handley, H. K., Turner, S., Macpherson, C., Gertisser, R. & Davidson, J. P. Hf–Nd isotope and trace element constraints on subduction zone inputs at island arcs: Limitations of Hf anomalies as sediment input indicators. *Earth Planet. Sci. Lett.* **304,** 212–223 (2011).
23. Mierdel, K., Keppler, H., Smyth, J. R. & Langenhorst, F. Water solubility in aluminous orthopyroxene and the origin of Earth's asthenosphere. *Science* **315,** 364–368 (2007).
24. Richard, M. *et al*. Geology of Mt. Iraya volcano and Batan island, northern Philippines. *Philipp. Bull. Volcanol.* **3,** 1–27 (1986).
25. Bell, D. R., Ihinger, P. D. & Rossman, G. R. Quantitative analysis of trace OH in garnet and pyroxenes. *Am. Mineral.* **80,** 465–474 (1995).
26. Hauri, E. H., Gaetani, G. A. & Green, T. H. Partitioning of water during melting of the Earth's upper mantle at H_2O-undersaturated conditions. *Earth Planet. Sci. Lett.* **248,** 715–734 (2006).
27. Beier, C., Turner, S., Sinton, J. & Gill, J. Influence of subducted components on back-arc melting dynamics in the Manus Basin. *Geochem. Geophys. Geosyst.* **11,** Q0AC03 (2010).
28. Engdahl, E. R., van der Hilst, R. & Buland, R. Global teleseismic earthquake relocation with improved travel times and procedures for depth determination. *Bull. Seismol. Soc. Am.* **88,** 722–743 (1998).
29. Green, D. H., Hibberson, W. O., Kovacs, I. & Rosenthal, A. Water and its influence on the lithosphere–asthenosphere boundary. *Nature* **467,** 448–452 (2010).
30. Williams, R. W. & Gill, J. B. Effects of partial melting on the uranium decay series. *Geochim. Cosmochim. Acta* **53,** 1607–1619 (1989).

Acknowledgements

We wish to thank the participants of the 2010 State of the Arc meeting on Santorini for their inspiration and discussions. We are grateful to I. Smith for the XRF analyses and to P. Wieland for analytical assistance at Macquarie. H. O'Neill first encouraged us to look at water and K. Grant helped with the initial FTIR scans. The original manuscript was greatly improved by comments from F. Huang. This work was funded by an Australian Research Council Professorial Fellowship (DP0988658) to S.T., a New Zealand Foundation for Research, Science and Technology post-doctoral Fellowship to M.T. and a National Science Foundation grant (OCE 0841075) to P.v.K. It used instrumentation funded by ARC LIEF and DEST Systemic Infrastructure Grants, Macquarie University and industry.

Author contributions

S.T. planned the project, carried out preliminary analyses and wrote the manuscript. J.C. carried out the majority of the U-series analyses. M.T. performed the FTIR work. P.v.K. carried out the geodynamic calculations. R.M. and G.P. provided the samples. M.S. produced the seismic images.

Additional information

The authors declare no competing financial interests. Supplementary information accompanies this paper on www.nature.com/naturegeoscience. Reprints and permissions information is available online at http://www.nature.com/reprints. Correspondence and requests for materials should be addressed to S.T.